# Mode Division Multiplexed Transmission over Elliptical Core Few Mode Fiber with Non-Degenerate LP11 Modes Using Mode Selective Coupler Based Multiplexers

Xin Chen[1], Jaekwon Ko[2], Jason E. Hurley[1], Jeffery S. Stone[1], Jae Hyeon Lee[2], Byoung Yoon Kim[2], and Ming-Jun Li[1]
*1. Corning Incorporated, Corning, NY 14831, USA*
*2. KS Photonics, Daejeon 34025, South Korea*
chenx2@corning.com

***Abstract*—Mode division multiplexed transmission is demonstrated over 500 m elliptical core few-mode fiber using multiplexer and de-multiplexer made from mode selective couplers with non-degenerate $LP_{11a}$ and $LP_{11b}$ modes at 25Gb/s over two of the channels.**

***Keywords— few-mode fiber, mode division multiplexing, mode selective coupler, elliptical core few-mode fiber***

## I. INTRODUCTION

To meet the ever-growing demands for more bandwidth and new applications, data transmission has moved to higher data rates with more overall capacity in optical communications. Current fiber-optic communication systems based on single-mode fiber are nearing their fundamental limit of ~100 Tb/s per fiber [1-2]. To address this challenge, extensive efforts have been made to develop the space division multiplexing (SDM) techniques based on multi-core fibers (MCFs) [3-4], and mode division multiplexing system (MDM) based on few-mode fibers (FMFs) and multimode fibers (MMFs) [5-7].

MDM systems use FMFs or MMFs, in which case each mode or mode group is a transmission channel, increasing the system capacity by a factor of N corresponding to the number of modes. For MDM transmission, mode coupling along the fiber causes signal crosstalk among different modes that degrade signal quality. To deal with the mode coupling issue, coherent detection and multiple-input-multiple output (MIMO) digital signal processing (DSP) are used to separate the channels [8-9]. However, the coherent detection and MIMO DSP significantly increase the system complexity, cost and power consumption, which are not desired for data center applications.

To enable the MDM transmission, high quality mode multiplexer (Mux) and de-multiplexer (DeMux) devices are critical components. Different approaches have been used to implement the Mux/DeMux either using phase plates [6] or mode selective couplers (MSCs) [10,11]. MSC using side-polished fibers is the main approach of interest to the current work, which is also a potentially low-cost approach. While much of the work in the literature has focused on long distance communications, our interest is at relatively short distances. In a recent paper [7], we utilized an 850-nm single-mode VCSEL as the laser source and reported MDM transmission over 1-km standard single-mode fiber, which is two-mode at 850 nm. Due to the circular symmetry of single-mode fibers, the $LP_{11a}$ and $LP_{11b}$ have nearly the same effective index and group delay. As a result, they can easily be coupled. To reduce mode coupling effects of $LP_{11}$ modes, an elliptical core (e-core) FMF has been proposed [12]. A similar idea has also been applied to ring core fiber design [13]. In the e-core FMF, the ellipticity of the core breaks the degeneracy of modes in a mode group of a circular core fiber, which reduces the mode coupling among these modes. Using an e-core FMF, MDM transmission of real-time 10GbE traffic using commercial SFP+ transceivers without coherent detection and MIMO-DSP was demonstrated over 0.5 km of fiber at 1310 nm. In [12] the Mux/DeMux were based on a free-space implementation. In this paper, we extended the work to use compact MSC based Mux/DeMux and demonstrate transmission at higher data rate using 25G LR transceivers. Section II presents the elliptical core fiber design concept and the detailed characterization of an e-core FMF. Section III presents the Mux/DeMux fabrication and characterization. Section IV shows the link characterization and transmission testing results. Finally, Section V presents the conclusions.

## II. ELLIPTICAL CORE FIBER WITH HIGH BIREFRINGENCE

### A. *E-core FMF with non-degenerate $LP_{11a}$ and $LP_{11b}$ modes*

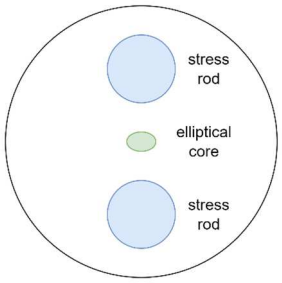


Fig. 1 Schematic of the elliptical core fiber with stress rods.

For fibers with circular cores, linearly polarized mode (LP mode) approximation is often used for simplicity. In the LP mode approximation, the true second higher order eigen-modes (TE01, TM01, HE21 modes) with donut-shape intensity distribution are regrouped to become the well-known $LP_{11even}$ (LP11a) and $LP_{11odd}$ (LP11b) modes with orthogonal intensity lobes. Since the true modes are not

exactly degenerate, the intensity lobes cannot be maintained as they propagate and are subject to environmental perturbations. As a result, an e-core fiber concept has been introduced [12]. The schematic layout of the elliptical core fiber is shown in Fig. 1.

In e-core fibers, the LP modes are true eigen-modes with lifted degeneracy resulting in the stability of the lobe intensity distributions [14, 15] illustrated in Fig. 2.

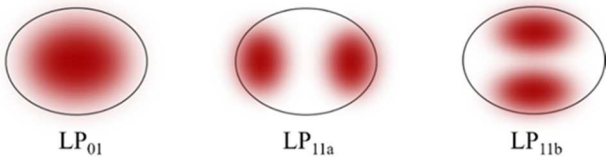


Fig. 2. Intensity distribution of lowest three modes, $LP_{01}$, $LP_{11a}$($LP_{11even}$), and $LP_{11b}$($LP_{11odd}$) in an elliptical core fiber.

The large difference in the propagation constants of two anti-symmetric modes ($LP_{11a}$ and $LP_{11b}$) provided by a large core eccentricity prevents coupling between the modes in the presence of external perturbations. The stability of lobe orientation in the e-core fiber greatly reduces the complexity not only for device fabrication but also for signal processing in mode-division multiplexed systems [16].

### *B. Characterization of the group delays of the e-core FMF*

The large difference in the propagation constants can be experimentally measured and verified. Such difference is exhibited by the group delay difference between $LP_{11a}$ and $LP_{11b}$ modes. In [17], a method for measuring the group delay of FMFs has been presented. Through a vector network analyzer (VNA) and proper E-O and O-E conversion the complex transfer function (CTF) over a frequency range for the fiber under test (FUT) at a given launch condition, which is also labelled as $S_{21}$, can be measured. In the current paper, we use a very similar experimental setup to measure the CTF of the FUT. Since the FUT is an FMF, we used a fiber alignment stage to control the relative offset between the launching single mode fiber and the FUT to be able to excite all guiding modes of the fiber. Also, a polarization controller is used to manipulate the state of polarization entering the FUT.

The CTF takes the form,

$$CTF(f) = S_{21}(f) = \sum_{j=1}^{n} a_j \cdot \exp(-i \cdot 2\pi f \tau_j), \quad (1)$$

where $a_j$ is the relative optical power in mode $j$, and $\tau_j$ is the group delay of mode $j$. Through proper calibration in the back-to-back condition with only a short piece of fiber of 20 cm, we can take out the contributions of the baseline system and obtain the CTF of the FUT only.

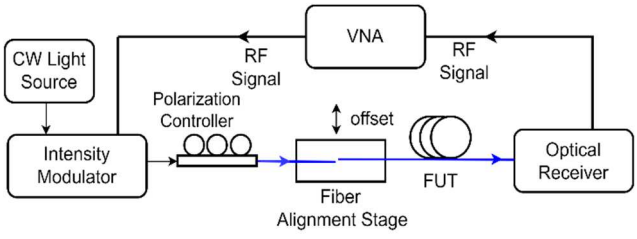


Fig. 3 Experimental setup for measuring the CTF of FUT.

One can perform an inverse Fourier transform of $CTF(f)$ on either the real or imaginary part to extract the time-domain information from the frequency domain measurement to obtain the group delay of each core, $\tau_j$. To fully resolve the time domain information without causing aliasing or ambiguity of the group delay time $\tau_j$, the sampling frequency step $df$ needs to meet the condition as set by Nyquist theorem, $df \leq \frac{1}{2 \cdot \max(\tau_1, \ldots \tau_n)}$, which results in unreasonable large numbers of points that need to be sampled. However, this problem can be solved if we apply a de-aliasing procedure that the peak value in the inversion Fourier transform is related to the actual group delay of each core $\tau_j$ by a simple equation,

$$\tau_j = k/df \pm t_j \quad (2)$$

where $k$ is an integer. Depending on the sign before $t_j$, the time sequence from inverse Fourier transform can either be the same time sequence or the opposite one compared to the actual propagation time for each core. With a proper choice of $k$ based on the fiber length and estimated group index information, we can recover the propagation time with right time sequence and can de-alias the signal to obtain the full group delay $\tau_j$ for each mode correctly. Detailed procedures have been described in [18] by assuming an input pulse and producing the output pulses from the FUT through processing the CTF into a slow varying version to a local time frame, called modified CTF. Subsequently the output pulse can be calculated. When proper value of $k$ and sign in Eq. (2) are chosen, well behaved output corresponding to the de-aliased condition can be identified. Since the fiber length information and the group delay per kilometer is typically known to very good accuracy, the initially estimated $k$ value is typically accurate to within +/- 1 so that the de-aliasing to recover the true group delay of each mode can be done relatively easily. Also, the frequency parameters, i.e., the range of frequency and the number of points (NOPs) of sampling used by VNA for measuring CTF can be chosen to further eliminate the ambiguity of identifying the de-aliased condition.

Using the experimental setup in Fig. 3, we have done measurements on 2-km of the e-core FMF. At the launch end, the excitation of the modes can be adjusted through an alignment stage which can control the relative offset between the launch single mode fiber and the FUT to ensure that all three modes of the fibers are significantly excited. The polarization controller can adjust the relative excitation between two polarization modes within each mode. It is important in the transmission experiment to reduce the impairment from polarization mode dispersion (PMD). In our measurement, we used the frequency range from 10 MHz to 12 GHz with 960 sampling points to obtain the CTF of the FUT with all three modes, $LP_{01}$, $LP_{11a}$ and $LP_{11b}$ excited. The inverse Fourier transform was first performed on the real part of CTF. The $k$ value in Eq. (2) was determined to be 122 and the peak values associated with each mode had a negative sign. Using an assumed optical input pulse whose FWHM pulse width was around 230 ps, we obtained output pulses as shown in FIG. 4, which correspond clearly to the three modes supported by the fiber. Through the use of the Muxes in the testing setup, we can determine which pulse corresponds to which mode as will be explained in Section III. The $LP_{01}$

mode has highest group delay while $LP_{11a}$ and $LP_{11b}$ have lower but separate group delays. Over the 2 km length of fiber, the group delays for $LP_{11a}$ and $LP_{11b}$ are separated by 2.46 ns.

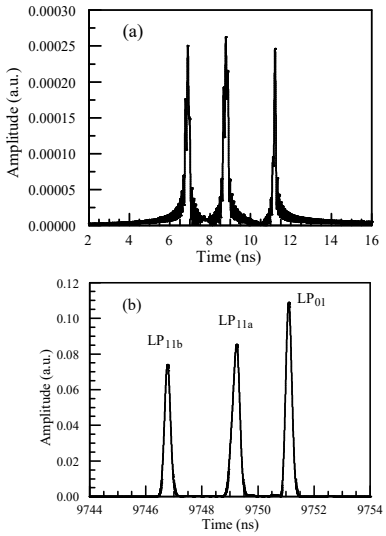


Fig. 4. (a) Inverse Fourier transform of the real part of CTF. (b) The calculated output pulses for 2-km of the e-core FMF.

## III. Mux and Demux Device Fabrication and Characterization

### A. Mux Device fabrication

Fig. 5. shows the configuration of the mode Mux implemented in this work. Signals from three single mode fibers are coupled to the three spatial modes ($LP_{01}$, $LP_{11a}$ and $LP_{11b}$) in an e-core fiber. For Channel 1 ($LP_{01}$ channel), the single mode fiber was directly spliced to the e-core fiber to excite the $LP_{01}$ mode in the e-core fiber. For Channel 2 ($LP_{11a}$ channel) and 3 ($LP_{11b}$ channel), cascaded MSC are used to excite $LP_{11a}$ and $LP_{11b}$ modes in the e-core fiber. The MSCs are based on evanescent field coupling between the side polished single mode fiber [11] and e-core fiber. A DeMux has an identical configuration as the Mux except that it operates in backward direction.

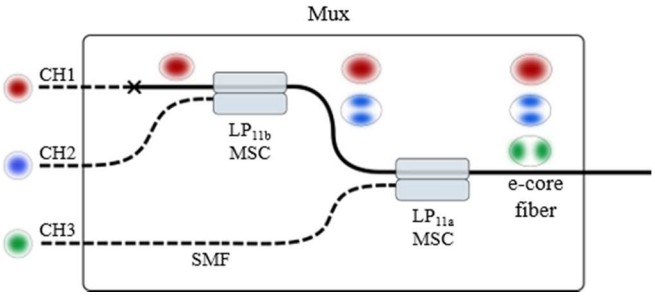


Fig. 5. Configuration of the Mux

Fig. 6 shows the structures of the MSCs for $LP_{11a}$ and $LP_{11b}$ modes. The orientations of the polished sides were determined by the symmetry of the core ellipse and the stress members to maximize mode overlap between the fibers [19]. We also measured the effective indices of $LP_{11a}$ and $LP_{11b}$ modes in the side-polished e-core fiber with the prism coupling method [10], and they were 1.4481 and 1.4474 at the wavelength of 1310 nm, respectively. The pairing single mode fibers were tapered so that the effective indices of the pairing modes were matched within ±0.0002.

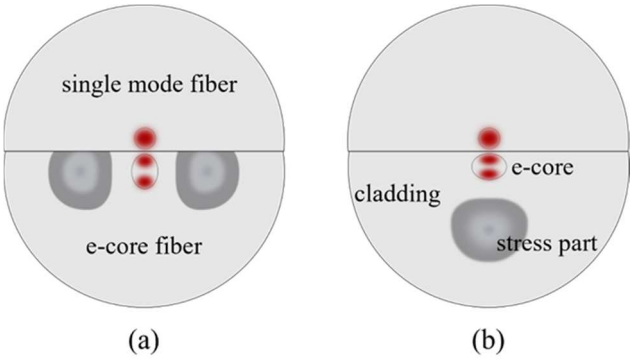


Fig. 6. Illustration for the structure of MSCs. (a) MSC for $LP_{11a}$ mode. The major axis of e-core is vertical to polishing surface. (b) MSC for $LP_{11b}$ mode. The major axis of e-core is horizontal to polishing surface.

### B. Insertion loss of the devices

We measured the output intensity profiles of the fabricated Muxes with a beam profiler. The two devices are labelled as 'Mux 1' and 'Mux 2' respectively. The results are shown in Fig. 7. The beam profiles are clearly what we expected for $LP_{01}$, $LP_{11a}$ and $LP_{11b}$ modes.

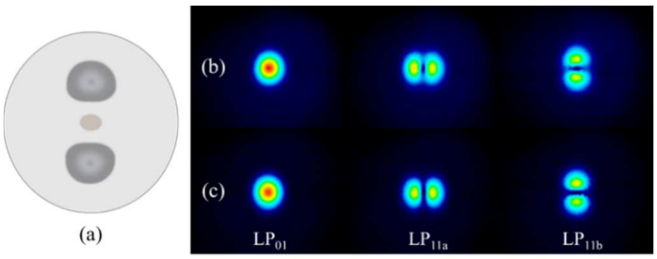


Fig. 7. (a) Cross-section of e-core fiber-end for reference; (b) Output intensity profile of the 'Mux 1'; (c) Output intensity profiles of the 'Mux 2'.

Table. 1. Measured insertion loss for two Muxes

Mux 1

| Mode | Insertion Loss (dB) | PDL (dB) |
|---|---|---|
| $LP_{01}$ | -0.36 | 0.05 |
| $LP_{11a}$ | -0.62 | 0.13 |
| $LP_{11b}$ | -1.35 | 0.38 |

Mux 2

| Mode | Insertion Loss (dB) | PDL (dB) |
|---|---|---|
| $LP_{01}$ | -0.46 | 0.05 |
| $LP_{11a}$ | -0.51 | 0.04 |
| $LP_{11b}$ | -1.20 | 0.66 |

The insertion losses of the devices are summarized in Table 1. In the subsequent link testing and transmission experiments done in Section IV, they are used in the setup near the transmitters and receivers respectively. $LP_{11b}$ mode channel of the Muxes showed relatively higher loss and polarization dependent loss (PDL) than the other channels because it experiences extra loss passing through $LP_{11a}$ leg of the MSC as can be seen in the Fig. 5. The values in the table are the worst case in various input polarization state.

## IV. Link Characterization and Transmission Experiment

In this section we conduct link level characterizations and present results of system level transmission experiments.

### A. Link characterization

Fig. 8 shows the link configuration. 'Mux 1' is used as the Mux near the transmitter. It combines the incoming signals from $LP_{01}$, $LP_{11a}$ and $LP_{11b}$ ports into the e-core FMF carrying all signals. 'Mux 2' is used as the DeMux near the receiver. Through DeMux, all signals in the e-core FMF are separated into three streams of signals into DeMux's $LP_{01}$, $LP_{11a}$ and $LP_{11b}$ output ports. The e-core FMF used for the link characterization and transmission experiment has a length of 500 m. Since the FMF is highly birefringent for each mode, it broadens the pulses carrying the transmission signals due to PMD. In [12] the 10G transmission was limited to the distance of 500 m. In the current work, by introducing a polarization controller before each incoming signal port, we are able to launch only one linear state of polarization, which helps to achieve higher data rate transmission at 25Gb/s.

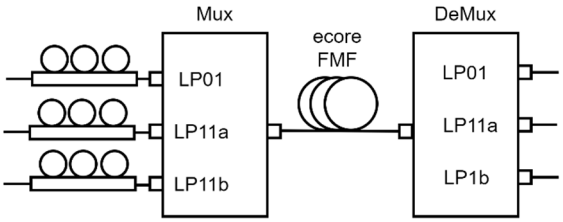


Fig. 8. The link configuration with Mux, DeMux and e-core FMF.

The insertion losses and crosstalks between different ports or channels with 500 m e-core FMF in the link have been measured. Table 2 shows the results. The diagonal cells show the link level insertion losses. It can be found that the $LP_{01}$ channel has the lowest link loss of 1.36 dB including the loss contributions from fiber attenuation, connector loss and insertion losses of the Muxes. $LP_{11a}$ and $LP_{11b}$ channels have higher losses of 2.06 dB and 3.76 dB. The crosstalks are shown in the off-diagonal cells of the table. The crosstalks from $LP_{01}$ mode to two other modes and from $LP_{11a}$ to two other modes are below -15 dB. The crosstalks from $LP_{11b}$ to $LP_{01}$ and $LP_{11a}$ are -17.76 dB and -11.36 dB respectively, with the later limiting the overall performance of the link.

The primary effort in preparing the link shown in Fig.8 was the fusion splicing of the e-core FMF of the main FUT with the e-core pigtail of the Mux and Demux. Due to slight manufacturing imperfection of the e-core FMF, the fiber is slightly non-uniform down the length, which caused difficulty in splicing the FMF together to minimize the insertion loss and crosstalk. We utilized a Vytran GPX3400 from Thorlabs Inc., an advanced splicer for splicing different types of fibers. We incorporated a combination of orientational alignment of the stress rods followed by active monitoring of the output optical powers before fusion splicing to optimize the insertion loss and crosstalk values are shown in Table 2.

During the preparation of the link shown in Fig. 8, we also measured the propagation delay in each arm for the Mux and Demux. Since the $LP_{01}$-to-$LP_{01}$ channel has the total propagation delay added from the $LP_{01}$ arm of the Mux and DeMux and the $LP_{01}$ propagation delay of the e-core FMF over 500 m, we could obtain the $LP_{01}$ group delay of 500 m e-core FMF alone by subtracting the delays from Mux and Demux. Similarly, we conducted measurements for the $LP_{11a}$ and $LP_{11b}$ channels. Through comparing the group delays we learned the time sequence of the three modes, which enabled us to label the modes associated with the group delay in Fig. 4(b).

Table 2. Insertion loss and crosstalk of the link for each channel in dB unit

| | DeMux: LP01 | DeMux: LP11a | DeMux: LP11b |
|---|---|---|---|
| Mux: LP01 | 1.36 | -18.46 | -15.66 |
| Mux: LP11a | -17.56 | 2.06 | -16.06 |
| Mux: LP11b | -17.76 | -11.36 | 3.76 |

### B. Transmission experiment

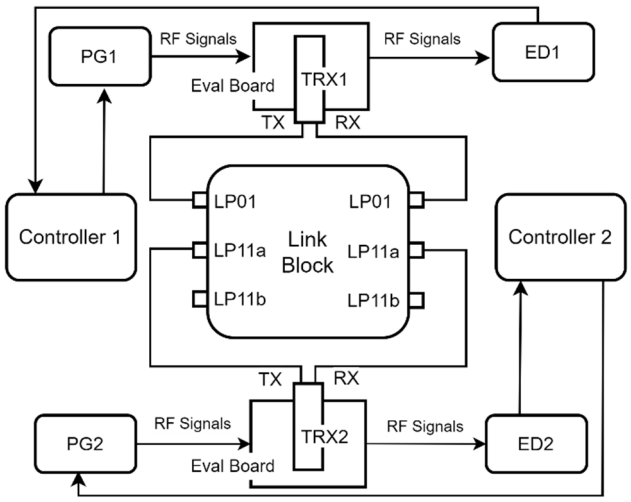


Fig. 9 The schematic of the transmission testing setup. The link block represents the whole link configuration in Fig. 8. PG is the pattern generator, ED is the error detector, and TRX is transceiver. Each pair of PD and ED is controlled by one controller.

With all the properties of the fibers, devices and link characterized, we then proceeded to conduct the transmission testing. The configuration of the full transmission experiment is shown in Fig. 9. In the transmission experiment, two sets of Agilent BERT system were used to measure the bit error rate (BER) for $LP_{01}$ channel and $LP_{11a}$ channel. The pattern generators (N4951B) were used to generate $2^{31}$-1 PRBS non-return-to-zero (NRZ) signals at the data rate of 25.78125 Gb/s to feed into $LP_{01}$ and $LP_{11a}$ channels. Two 25G LR transceivers were used. The 25G LR transceivers are single mode transceivers rated for 10 km transmission over standard single mode fibers. Each transceiver was plugged into an evaluation board, from which the transmitter (Tx) side signals and receiver (Rx) side signals were connected with the pattern generator (PG) and error detector (ED) respectively. The output optical signals from either $LP_{01}$ and $LP_{11a}$ output port were detected by the transceivers' built-in receivers and the errors were counted by Agilent error detector (N4952A-E32). The transmission over $LP_{01}$ and $LP_{11a}$ channels was done simultaneously. The polarization controller for each channel is adjusted to minimize the PMD for each channel. Since the e-core FMF has high birefringence and high PMD, the use of polarization controller is very helpful to improve the transmission performance. During the adjustments, we actively observed and monitored the eye diagram quality and could see that the quality of the eye diagram got significantly improved due to excitation of only one polarization.

The bit error rate (BER) for $LP_{01}$ channel was $4.3\times10^{-10}$ over 5 mins of testing while the $LP_{11a}$ channel achieved

$3.1\times10^{-9}$ BER over the same duration. The eye diagrams for the two channels at both the back-to-back condition and with 500 m e-core FMF are shown in Fig. 10. It can be found that the eye diagrams get degraded relative to the eye diagrams based on the input signals for $LP_{01}$ and $LP_{11a}$ channels. But the eye diagrams are still open, which is consistent with the observed BER performance. It should be noted that the transmission quality is significantly affected by the crosstalk between different channels. The signals from one channel tunneled into another channel would degrade the performance of another channel significant if the crosstalk is significant. In Section IV A, we showed the crosstalk at the link level for all channels and identified that the crosstalk from $LP_{11b}$ to $LP_{11a}$ channel is the limiting factor. In our initial experiment when all channels were actively driven from three 25G LR transceivers, we found that the crosstalk signals from $LP_{11b}$ were too detrimental so that we ended up doing the transmission experiment without using $LP_{11b}$ channel. We noted in Section IV A, the cause for high crosstalk was from slightly non-uniform fiber resulting in non-optimal splicing quality. It is not a limitation of the presented fiber mechanism and Mux making principle.

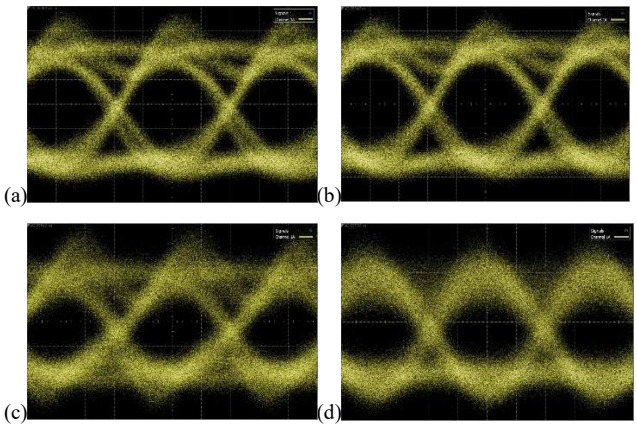


Fig. 10. The eye diagrams for (a) input signals for $LP_{01}$ channel; (b)input signals for $LP_{11a}$ channel; (c) output signals for $LP_{01}$ channel with 500 m e-core FMF; (d) output signals for LP01 channel with 500 m e-core FMF.

## V. Conclusions

E-core FMF fiber with non-degenerate $LP_{11a}$ and $LP_{11b}$ mode enables making coupler based MSCs to handle the $LP_{11a}$ and $LP_{11b}$ as separate channels. The MSCs can be made based on evanescent field coupling between the side polished single mode fiber and e-core fiber. Two Muxes were fabricated and packaged in a compact box, one of which was used as Mux and another one was used as DeMux. For Channel 1, the single mode fiber was directly spliced to the e-core fiber to excite the $LP_{01}$ mode in the e-core fiber. For Channel 2 and 3, cascaded mode selective couplers (MSC) are used to excite $LP_{11a}$ and $LP_{11b}$ modes in the e-core fiber. Detailed performance parameters such as insertion loss and PDL have been measured for each channel. Applying a recently developed method [17-18] of measuring group delay to the e-core fiber, we observed three modes, $LP_{01}$, $LP_{11a}$ and $LP_{11b}$ with distinct group delay values. Facilitated by the Mux and Demux with the measurement method, we were able to identify the individual group delay associated with the specific mode. The link loss and crosstalk have been measured. The MDM transmission performance was strongly influenced by crosstalk, as is expected in general for all MDM schemes. We demonstrated successful transmission over $LP_{01}$ and $LP_{11a}$ channels simultaneously after idling the $LP_{11b}$, which had a relatively high crosstalk over $LP_{11a}$ channel. Further experimental efforts will be made to improve the crosstalk performance and transmission over all three channels simultaneously.

## References


[1] R. Essiambre, et al., "Capacity limits of optical fiber networks," J. Lightwave Technol. 28 (4) 662–701, (2010).

[2] R. Essiambre, R.W. Tkach, "Capacity trends and limits of optical communication networks," Proc. IEEE 100 (5) 1035–1055, (2012).

[3] K. Imamura, K. Mukasa, T. Yagi, "Investigation on multi-core fibers with large Aeff and low micro bending loss," in: Optical Fiber Communications Conference 2010, San Diego, March 2010, Paper OWK6.

[4] T. Hayashi, T. Nagashima, O. Shimakawa, T. Sasaki, E. Sasaoka, "Crosstalk variation of multi-core fibre due to fibre bend," in: ECOC 2010, Turin, September 2010, Paper We.8.F.6.

[5] Y. Jung, et al., "Low-loss 25.3 km few-mode ring-core fiber for mode-division multiplexed transmission," J. Lightwave Technol. 35 (8) 1363–1368, (2017).

[6] G. Labroille, et al., "30 Gbit/s transmission over 1 km of conventional multi-mode fiber using mode group multiplexing with OOK modulation and direct detection," in ECOC (2015).

[7] Kangmei Li, Xin Chen, Jaekwon Ko, Jason E. Hurley, Jeffery S. Stone, Kyung Jun Park, Byoung Yoon Kim, and Ming-Jun Li. "Mode division multiplexed 850-nm single-mode VCSEL transmission using standard single-mode fiber." IEEE Photonics Technology Letters 33, (22) 1231-1234, (2021).

[8] T. Sakamoto, et al., "Low-loss and Low-DMD few-mode multi-core fiber with highest core multiplicity factor," in: 2016 Optical Fiber Communications Conference and Exhibition, OFC, 2016

[9] Y. Sasaki, et al., "Few-mode multicore fiber with 36 spatial modes (Three modes (LP 01, LP 11a, LP 11b) × 12 cores)," J. Lightwave Technol. 33 (5) 964–970, (2015)

[10] W. V. Sorin et al., "Highly selective evanescent modal filter for two-mode optical fibers," Opt. Lett. 11(9), 581-583 (1986).

[11] Kyung Jun Park *et al.,* "Broadband Mode Division Multiplexer Using All-Fiber Mode Selective Couplers," Optics Express 24, (4) 3543–49, (2016).

[12] Ezra Ip, Giovanni Milione, Ming-Jun Li, Neda Cvijetic, Konstantinos Kanonakis, Jeffery Stone, Gaozhu Peng et al. "SDM transmission of real-time 10GbE traffic using commercial SFP+ transceivers over 0.5 km elliptical-core few-mode fiber," Optics express 23, (13) 17120-17126, (2015).

[13] Weijun Song, Hongyao Chen, Jianping Wang, Changling Liu, Yijin Chen, Zizheng Li, and Mei Liu. "Panda type elliptical ring core few-mode fiber." Optical Fiber Technology 60 (2020): 102361.

[14] Allan W. Snyder and Xue-Heng Zheng, "Optical Fibers of Arbitrary Cross Sections," JOSA A 3, (5) 600–609, (1986).

[15] B. Y. Kim *et al*., "Use of Highly Elliptical Core Fibers for Two-Mode Fiber Devices," Optics Letters 12, (9) 729–31, (1987).

[16] Koji Igarashi *et al.,* "All-Fiber-Based Selective Mode Multiplexer and Demultiplexer for Weakly-Coupled Mode-Division Multiplexed Systems," Optics Communications, 408, 58–62, (2018).

[17] Kangmei Li, Xin Chen, Jason Hurley, Jeffery Stone, and Ming-Jun Li. "Measuring modal delays of few-mode fibers using frequency-domain method." Optical Fiber Technology 62, 102474, (2021).

[18] Xin Chen, Kangmei Li, Jason E. Hurley, Ming-Jun Li,"Differential mode delay and modal bandwidth measurements of multimode fibers using frequency-domain method," Optical Fiber Technology, 72, 102998, (2022).

[19] John D. Love and Nicolas Riesen, "Mode-Selective Couplers for Few-Mode Optical Fiber Networks," Optics Letters 37, (19) 3990–92, (2012).